

# Network Structure and Properties of Polyurethanes from Soybean Oil

Zoran S. Petrović, Liting Yang,\* Alisa Zlatanić, Wei Zhang, Ivan Javni

Kansas Polymer Research Center, Pittsburg State University, Pittsburg, Kansas 66762

Received 16 December 2006; accepted 8 February 2007

DOI 10.1002/app.26346

Published online 14 May 2007 in Wiley InterScience (www.interscience.wiley.com).

**ABSTRACT:** Vegetable oils are very heterogeneous materials with a wide distribution of triacylglycerol structures and double-bond contents. The hydrogenation of epoxidized soybean oil (ESO) produces polyols having a functionality distribution related to that of soybean oil. Therefore, these polyols are convenient substances for studying the impact of structural heterogeneity on network formation and properties. Polyols of hydroxyl numbers ranging from 225 to 82 mg KOH/g and weight-average functionalities ranging from 4.4 to 2.7 were obtained by the variation of the time of hydrogenation of ESO. An analysis of the functionality distribution in polyols shows that gel points with diisocyanates vary

from 54 to 76% conversion. The molecular weights of the network chains of polyurethanes prepared from these polyols and diphenyl methane diisocyanate varied from 688 to 1993. Polyols with hydroxyl numbers above 200 mg KOH/g gave glassy polymers, whereas those below that value gave rubbers. The heterogeneity of polyols had a negative effect on the elastic properties only at low crosslinking densities. © 2007 Wiley Periodicals, Inc. *J Appl Polym Sci* 105: 2717–2727, 2007

**Key words:** biopolymers; networks; polyurethanes; renewable resources; structure-property relations

## INTRODUCTION

Vegetable-oil-based polyurethanes are a class of materials from renewable resources with some very promising competitive advantages, such as hydrophobicity, higher thermooxidative stability, and favorable prices. Vegetable oils and soybean oil (SBO), in particular, are very heterogeneous materials, and when they are converted to polyols this heterogeneity may even increase. The nature and degree of heterogeneity should be understood to find proper applications for these new materials. An experimental analysis of the structure of oils is difficult and time-consuming, but it has been done by several researchers.<sup>1,2</sup> The experimental analysis of the heterogeneity of polyols would be even more complex and virtually impossible in a reasonable time frame. Instead, we have applied a simulation to gain insight into the distribution of functional species and crosslinking behavior of new polyols. We previously developed a range of polyols from vegetable oils, using various methods, such as epoxidation,<sup>3,4</sup> hydroformylation,<sup>5</sup> and ozonolysis.<sup>6</sup> Because of the high functionality, these polyols can also be crosslinked with diisocyanates to give rigid

polyurethanes. The polymer properties are controlled by the crosslinking density as well as the structures of the polyols<sup>4</sup> and isocyanates.<sup>7</sup> This time, we have used the hydrogenation of epoxidized soybean oil (ESO) to obtain a family of polyols with different properties.

The hydrogenation of ESO is a direct and clean way of obtaining low-viscosity polyols with a narrow molecular weight distribution. Earlier, we found that a fully hydrogenated epoxidized soybean polyol crystallizes easily to give a low-melting-point grease.<sup>3</sup> However, the crystallization is also a function of the degree of hydroxylation, and one of the objectives of this work is to discern the relationship between the degree of hydrogenation, the physical state and properties of polyols, and the properties of urethane networks from these polyols. Because epoxidation and hydrogenation do not alter the distribution of functional groups, these polyols are useful for studying the effect of heterogeneity on properties. All polyols were fully characterized by spectroscopic techniques and by the measurement of the viscosity, hydroxyl (KOH/g) number, and epoxy content. Gel permeation chromatography (GPC) was used to determine the molecular weight distribution. The polyols were reacted with pure 4,4'-diphenyl methane diisocyanate (MDI) to obtain polyurethanes of different compositions and crosslinking densities. Swelling in toluene was used to estimate the crosslinking density. Differential scanning calorimetry (DSC) and dynamic mechanical analysis (DMA) were used to determine the glass transitions and moduli versus the temperature.

\*Present address: College of Chemistry and Environment, South China Normal University, Guangzhou, 510631, People's Republic of China.

Correspondence to: Z. Petrovic (zpetrovi@pittstate.edu).

Mechanical tests were used to determine the strength and rigidity of the polymers. The thermal stabilities of polyurethanes were compared through thermogravimetric analysis (TGA) tests of all samples.

## EXPERIMENTAL

### Materials

The epoxidized vegetable oil used was Flexol from Union Carbide (Danbury, CT; now Dow Chemical). The measured epoxy oxygen content (EOC) was 6.7%. The specifications gave an iodine number of 1.0 g of I<sub>2</sub>/100 g, an acid number of 0.2 mg of KOH/g, an OH value of 5 mg KOH/g, a viscosity of 188 cSt at 37.8°C (100°F), and a specific gravity of 0.992.

Isopropyl alcohol (histology-grade), benzene, and toluene were obtained from Fisher Scientific (Pittsburgh, PA). Hydrogen gas was obtained from Air Products (Allentown, PA). Mondur M (pure MDI) was supplied by Bayer (Pittsburgh, PA) and was purified by vacuum distillation at 170°C shortly before use.

### Methods

The IR spectra were recorded on a PerkinElmer Spectrum 1000 Fourier transform infrared (FTIR) spectrometer (PerkinElmer, Waltham, MA). Samples were prepared as thin films on KBr or NaCl salt plates. The GPC chromatograms were obtained on a Waters system (Waters Corp., Milford, MA) consisting of a 510 pump and a 410 differential refractometer. Tetrahydrofuran was used as an eluent at 1.00 mL/min at 30°C. Four Phenogel columns plus a guard Phenogel column from Phenomenex (Phenomenex Corp., Torrance, CA) covering a molecular weight range of 10<sup>2</sup> to 5 × 10<sup>5</sup> were used. The viscosities were measured on a Rheometrics SR-500 dynamic stress rheometer (Rheometrics, Piscataway, NJ) between two parallel plates 25 mm in diameter with a gap of 1 mm. The OH values of the polyols were determined according to the ASTM E 1899-02 standard test method for OH groups through a reaction with *p*-toluenesulfonyl isocyanate and potentiometric titration with tetrabutylammonium hydroxide. The EOC in the polyols was determined by the direct titration of epoxy groups with HBr according to the standard method for oils and fats.<sup>8</sup>

A thermal analysis system from TA Instruments (New Castle, DE), consisting of a 3100 controller with a DSC 2910 module and a TGA 2050 module, was used to measure the glass transition and thermal stability. Dynamic mechanical tests were carried out on DMA 2980 from TA Instruments at 10 Hz and a heating rate of 5°C/min. The heating rate with DSC and TGA was 10°C/min. The tensile properties were measured on five specimens for each sample, at an

extension rate of 100%/min, according to ASTM D 882-97 with a tensile tester model 4467 from Instron (Canton, MA). Swelling experiments were performed on round or square, 1–2-mm-thick samples weighing between 0.2 and 0.5 g. The samples were immersed in 30 mL of toluene for 3 months at 25°C. The sample weight was measured periodically, and the change with time was recorded. After reaching the maximum weight, the samples started losing weight because of the extraction of the sol fraction until constant values were obtained. The solvent was replaced three times after the maximum swelling was obtained. The samples were dried, and the weight of the gel fraction was recorded. The sol fraction was the difference between the initial weight and gel weight divided by the initial weight expressed as a percentage. The degree of swelling (*Q*) was expressed as the ratio of the volume of the swollen sample at equilibrium (*V<sub>s</sub>*) to the volume of the gel fraction (*V<sub>0</sub>*). The volumes were calculated from the mass and densities of the polymer and solvents:

$$Q = V_s/V_0 = V_s/(W_0/\rho_2) \quad (1)$$

$$V_s = (W_0/\rho_2) + (W_s - W_0)/\rho_1 \quad (2)$$

where *W<sub>s</sub>* is the mass of the swollen sample; *W<sub>0</sub>* is the mass of the gel fraction obtained after drying; and  $\rho_1$  and  $\rho_2$  are the densities of the solvent and polymer, respectively. The two samples prepared with the lowest OH numbers were also swollen in dimethylformamide to check their solubility, but they were not soluble.

### Preparation of the polyol by hydrogenation of ESO

The polyol with the complete conversion of epoxy groups to OHs was prepared separately. The reaction was carried out in a Parr high-pressure minireactor (Parr Instrument Co., Moline, IL) (450 mL) equipped with temperature and stirrer-speed controls and a liquid sampling outlet. A mixture of ESO (50 g, 0.22 mol of epoxy group), isopropyl alcohol (50 mL), and 20% Raney nickel (wet, 10.0 g) was pressurized to 4 MPa (600 psig) of hydrogen at 25°C. It was then heated to 110°C and stirred for 5 h. The pressure was maintained at 3.4–6.9 MPa (500–1000 psig). The mixture was cooled to room temperature and filtered through Celite. The solvent was removed on a rotary evaporator, yielding a white wax with a melting point of about 58°C. The product, designated as fully hydrogenated, had an OH number of 225 mg KOH/g and a viscosity of 0.3 Pa s at 60°C. FTIR showed no residual epoxy groups, whereas the GPC trace showed a single peak. A small amount of dimer, observed at 30.5 min, was from the original ESO.

All other polyols were prepared with 5% catalyst to slow down the reaction. Samples were taken at different hydrogenation times, and the OH number and

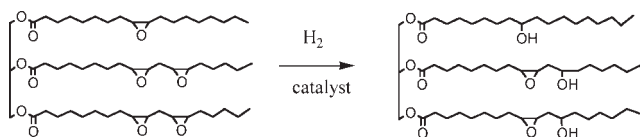


**Figure 1** Possible structure of a polyol obtained by the partial hydrogenation of ESO.

EOC of the samples were measured. The molecular weights and chemical compositions of the polyols, listed in Table A.I (in the appendix), were calculated from measured OH numbers and the starting EOC with the method explained in the appendix. The properties of the polyols are discussed in the next section.

### Polyurethanes from hydrogenated ESO polyols

Seven polyurethanes were prepared through the reaction of polyols with a 2% molar excess of distilled MDI. The components were heated to 70°C, mixed, and poured into a preheated mold to make 100 × 100 × 1 mm<sup>3</sup> sheets. The samples were kept in an oven at 110°C overnight (~ 15 h) to complete the cure. Polyurethane from the polyol obtained after 0.25 h of hydrogenation (OH number = 43 mg KOH/g) was a tacky, soft solid and was not tested.

## RESULTS AND DISCUSSION

The reaction for the preparation of polyols by the hydrogenation of ESO is shown in Figure 1. Within the literature, there are very limited reports on polyols by the hydrogenation<sup>9–14</sup> of epoxidized oil and practically no references on polyurethanes based on the polyols. SBO has on average about 4.6 double bonds per molecule, which can be converted to the same number of epoxy groups and as many OH groups by the hydrogenation of ESO. Residual epoxy groups are relatively rigid, causing moderate increases in the viscosity of polyols (the viscosity of ESO is typically ca. 220 mPa s vs 60 mPa s for SBO) and may have a positive effect on the modulus of polyurethane networks. However, their beneficial effect is mainly in increasing the thermal stability of the materials.<sup>15,16</sup> Several studies have proposed the use of polyols and prepolymers from vegetable oils with residual epoxy groups for the development of novel urethane products.<sup>15,17,18</sup> The structure of polyols from hydrogenated ESO is very complex and reflects the composition of SBO and the degree of hydroxylation. SBO consists of triacylglycerols of five major fatty acids. It contains about 15% saturated fatty acids [palmitic (P) and stearic (S)], or, on average, one fatty acid in two triacylglycerol molecules is expected to have no double bonds and therefore cannot be epoxidized. SBO contains about 25% oleic acid (O), which has one double bond and can

bear only one epoxy group. Linoleic acid (L) with two double bonds is the most abundant fatty acid with about 50%, whereas linolenic (Ln) with three double bonds is present at 5–8%. The degree of epoxidation of industrial ESO is usually above 90%. The starting ESO in this work had on average about 4.0 epoxy groups per triacylglycerol. The composition of triacylglycerol species in SBO is dominated by the presence of LLL (19%), LLO (15%), LLLn (10%), LOP (9%), OLO (6%), and OLLn (6%).<sup>1</sup> List et al.<sup>2</sup> reported somewhat different numbers [LLL (17.2%), LLO (17.9%), LLS (16.1%), LnLL (6.3%), LnLO (5.0%), LOS (11.9%), and OOO (3.1%)], whereas a host of other combinations are present in lower concentrations. On average, two triacylglycerol branches would have one epoxy, and the third would have two epoxy groups, but in reality, there are about 35 different combinations with zero to nine double bonds per triacylglycerol. Figure 2 shows that the most abundant fraction in SBO contains four double bonds (and when epoxidized would give four epoxy groups), one- and eight-double-bond triacylglycerols are present below 1%, whereas there are no nine-double-bond species.

When SBO is epoxidized, some loss of functional groups occurs (by ca. 15% in our case), but we can assume that the ratio between different triacylglycerol constituents will be retained. The structure of the species with a given number of functional groups also varies. For example, a triacylglycerol with three epoxy groups can have all three groups in one of the fatty acids, and two fatty acids will have no such groups as in LnSS. Other possibilities are fatty acids with two, one, or zero epoxy groups, as in epoxidized LOS, or all three fatty acids with one functional group, as in an OOO combination. The last case is the most desirable

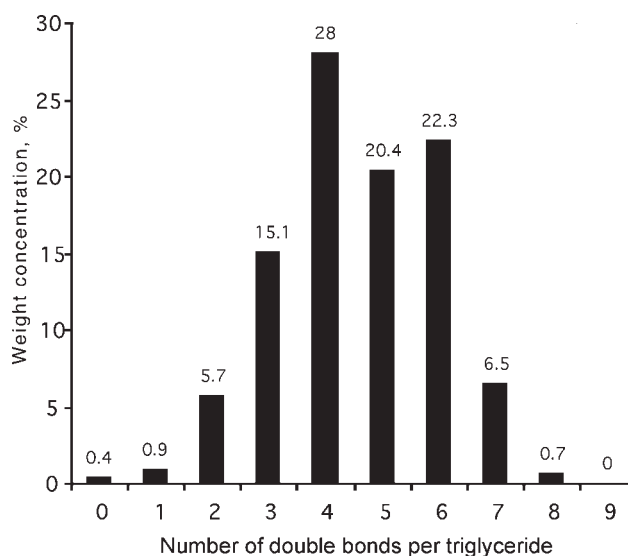


**Figure 2** Distribution of the number of double bonds per triacylglycerol in SBO based on the composition reported in ref. 2.

because all three chains would participate in the network structure equally, whereas LnSS would give us two saturated fatty acids as dangling chains, and LOS introduces one dangling chain. LnSS is present at only 0.1%, OOO is present at 3.1%, and LOS is present at 11.9%. In fact, in the SBO composition described previously, 38% of triacylglycerols have at least one saturated fatty acid in their structure. Dangling chains act as internal plasticizers, lowering the glass-transition temperature ( $T_g$ ) of the networks.<sup>19,20</sup> All this illustrates the complexity of the networks based on vegetable oils. When partial hydrogenation is carried out, the complexity increases because for each average OH group content, a wide distribution of functionalities is present. In the case of polyols having on average one functional group, significant nonfunctional triacylglycerols must be present to compensate for the presence of higher functional species. Nonfunctional material does not affect the real functionality of the system because zero-functional species are just solvents or plasticizers. Monofunctional species are detrimental to the network formation because they act as chain terminators. Two monofunctional polyols could react with diisocyanate to give a solvent-extractable trimer, but higher extractable oligomers can also be formed from several monofunctional molecules in combinations with di- and trifunctional polyols and diisocyanates. The presence of polyols of different functionalities results in the distribution of crosslinking densities in polyurethanes. Such materials usually display a broad glass transition as a result of superimposed glass transitions of network sections with low, medium, and high crosslinking densities. The fundamental question is how heterogeneity in functional species and reactive groups that are not at the end of the fatty acid chains affect the properties.

### Properties of polyols with different OH values

There are several sources of heterogeneity listed here. Heterogeneity in functionality distribution is observed even in the case of equal number of functional groups per triacylglycerol, arising from the position of the functional groups, as illustrated in Figure 3. The figure shows that three oleic acids (OOO) give even spacing between OH groups, whereas in the linoleic-oleic-saturated (LOS) combination, two groups are close, and

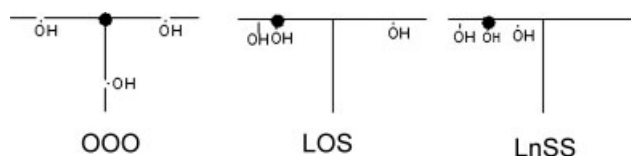


**Figure 3** Heterogeneity in the distribution of functional groups in a trifunctional triacylglycerol. The black spots designate the branching points.

the third is at a distance. In the case of a linolenic-saturated-saturated (LnSS) triacylglycerol, three groups are close, giving a high crosslinking density, similar to that of glycerin, with two saturated fatty acids as dangling chains that have no effect on the elastic properties of the network.

Heterogeneity in the number of functional groups per triacylglycerol exists because of the range of functionalities from 0 to 9, as in the original oil shown in Figure 2. Heterogeneity in the position of functional groups exists because OH groups can be located in oleic (hydroxy stearic) acid at the 9th or 10th carbon, in linoleic acid at the 9th or 10th and 12th or 13th, and in linolenic acid at the 9th or 10th, 12th or 13th, and 16th or 17th.

### Polyol functionality analysis and functionality determination

The functionality of polyols is important because it affects the gel point as well as the properties of networks. There is a great deal of confusion in the literature concerning the functionality of polyols. The functionality of a mixture of species of different functionalities is an average number. The usual averages used in polymer chemistry are the number average (first moment of distribution), weight average (second moment of distribution), and higher averages such as the z-average (third moment). The number-average functionality ( $f_n$ ) and weight-average functionality ( $f_w$ ) are defined as follows:

$$f_n = (\sum N_i \times f_i) / (\sum N_i) \quad (3)$$

$$f_w = (\sum N_i \times f_i^2) / (\sum N_i \times f_i) \quad (4)$$

where  $N_i$  is the number of moles of component  $i$  and  $f_i$  is the functionality of component  $i$ .

$f_n$  can be obtained experimentally by the division of the number-average molecular weight ( $M_n$ ; e.g., measured by vapor pressure osmometry) by the OH equivalent ( $E_{OH}$ ).  $E_{OH}$  can be calculated from the OH number ( $E_{OH} = 56,110/\text{OH number}$ ). The gel point correlates with  $f_w$ , and thus it is the most important parameter for the gelation process.  $f_w$  cannot be easily obtained if the exact composition and functionality of the species are not known.

### Structures of polyols with different OH contents

To predict the properties of polyols, gel points, and properties of polymer networks, it is necessary to know the compositions of different functional species in the polyols. The composition of the SBO fully converted to polyols is deduced from the composition of the starting oil. Assuming the SBO composition from ref. 2, we can calculate the composition of this polyol. Although the epoxidized oil used in this work was probably from a different SBO composition, the justifi-

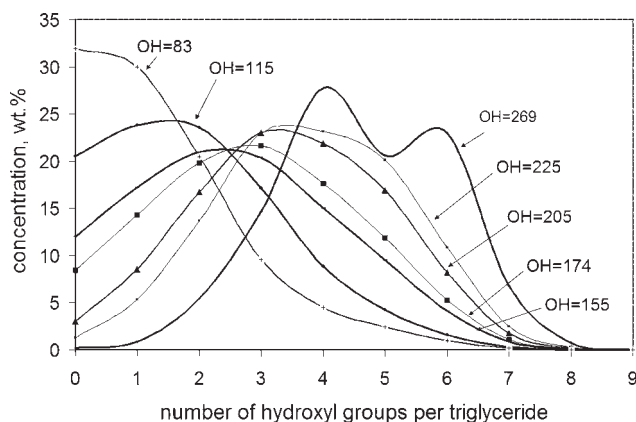


**Figure 4** Calculated distribution of functional species in polyols of different OH numbers.

cation for using the one from ref. 2 is that the variation in the composition of North American SBOs is not large enough to affect the main conclusions of this work. Besides, there are not many well-documented and detailed analyses of triacylglycerols in SBO. The initial SBO had on average 4.6 double bonds per triacylglycerol. If all double bonds were epoxidized and converted to OHs, the concentrations of components with different functionalities would be slightly changed because of the higher molecular weight of species with higher OH contents. We have applied a certain algorithm explained in the appendix to calculate the composition of the polyols from the composition of the original oil. The distribution of functional species in polyols calculated by this method is given in Table A.II in the appendix. Only the composition of the polyol of fully epoxidized and quantitatively hydrogenated SBO, which has the distribution of SBO in ref. 2, is certain. This exercise allowed us to calculate polyol properties such as  $f_w$ , predict the gel point with difunctional isocyanates, and determine the network parameters. Table A.I (in the appendix) shows that the  $M_n$  and weight-average molecular weight ( $M_w$ ) values are almost identical for all distributions, about 940 mg KOH/g. This value was taken for further calculations. The calculated functionalities of polyols presented in Table A.II vary from 2.7 to 5 (weight-average) or from 1.4 to 4.6 (number-average).

Because  $f_w$  of our polyols is always greater than 2, all systems would form a gel, which was experimentally proven. The calculated gel points in the absence of internal cyclization shift from 50 to 76% conversion for the samples with OH numbers of 269 and 82 mg KOH/g, respectively. In comparison with 71% conversion for standard trifunctional petrochemical polyols, most of our polyols have stronger crosslinking power. It is, however, well known that cyclization does take place and shifts gel points to somewhat higher conversions. We have found that the gel point in model systems shifted by about 3% to higher conversions.

The distribution of species of different functionalities in polyols is visualized in Figure 4. It shows that the species with functionalities of 4, 5, and 6, dominating the original polyol, are reduced, whereas the content of lower functionality species increases with a decreasing OH number for the polyols. Monofunctional species are the dominating fraction in the polyol with an OH number of 115, whereas nonfunctional species constitute 32% of the mass in the polyol with an OH number of 82 mg KOH/g. The nonfunctional species may act as plasticizers (solvent) in the final polymer, but they affect the network structure much less than monofunctional species. Their effect is expressed through dilution because it is known from gelation theory that networks formed in solution have a lower crosslinking density than when prepared in bulk.<sup>21,22</sup> Note that  $f_w$  is 8–100% higher than  $f_n$ , and the difference is higher in polyols with lower OH numbers. The gel points shown in Table A.II were calculated for 100% conversion in the stoichiometric polyol/diisocyanate systems and in the absence of cyclization. The sample with an OH number of 269 mg KOH/g is a reference with the theoretical maximum of OH groups that could be obtained from the oil composition given in ref. 2. It could not be prepared from the ESO used in this work.

IR spectra of polyols show decreasing epoxy peaks at 824 and 845  $\text{cm}^{-1}$  and an increasing OH peak at 3369  $\text{cm}^{-1}$  as the reaction time increases.

GPC curves in Figure 5 shift to the left with the reaction time. Large shifts in peaks to the left with the degree of hydrogenation cannot be caused by the increase in the molecular weight, which is very small, but rather are caused by the changes in the spatial configuration of triacylglycerol molecules in the solvent. The shift seems to be primarily driven by the disappearance of epoxy groups rather than the formation of OHs. It has been observed that the peak of ESO

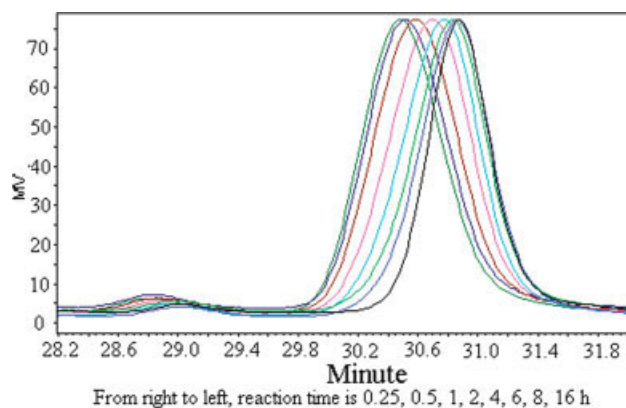


**Figure 5** GPC curves of polyols prepared at different reaction times. The shift of the GPC curves to the left is a result of increased hydroxylation. [Color figure can be viewed in the online issue, which is available at [www.interscience.wiley.com](http://www.interscience.wiley.com).]

TABLE I  
Chemical and Physical Properties of the Polyols

Reaction time (h)	EOC (%)	OH number (mg KOH/g)	Polyol functionality <sup>a</sup>	Viscosity at 25°C (Pa s)	Viscosity at 50°C (Pa s)	Highest melting point (°C)
0.25	5.59	43.2	0.7	0.43	0.15	35.0
0.5	5.05	55.7	0.9	0.48	0.16	37.9
1	4.34	81.6	1.4	0.58	0.19	45.6
2	3.25	115	1.9	0.86	0.23	54.1
4	2.02	154	2.6	solid	0.35	51.5
6	1.36	174	2.9	solid	0.58	51.6
16	0.55	206	3.5	solid	3.10 <sup>b</sup>	57.6
Fully hydrogenated	0.3	225	3.8	solid	0.3 at 60°C	58.3

<sup>a</sup>  $f_w$ .

<sup>b</sup> The sample crystallized in the rheometer.

would appear to the right of the peak for pure oil despite the increased molecular weight, whereas the hydrogenation of ESO would cause the shift to the left of the oil peak. This indicates that epoxidation creates smaller coils in tetrahydrofuran than oil because of the effect of epoxy groups on chain conformation.

No hydrolysis products such as diglycerides or free fatty acids were detected (no peaks on the right side of the main peak). The properties of the polyols are summarized in Table I. The polyols are cloudy liquids when the OH number is lower than 115 mg KOH/g. The viscosities measured at 50°C are very low and increase with increasing OH numbers.

All polyols and ESO crystallize. The highest melting points listed in Table I increase with an increasing degree of hydroxylation. DSC of the polyols shows multiple melting peaks suggesting the existence of different crystalline structures possibly containing different numbers of OH groups. Polyols with low OH numbers have considerable amounts of unreacted ESO, which displays a characteristic melting pattern. Complex melting behavior is a result of the complex mixture of crystallizing species in these polyols. The fully hydrogenated ESO has a single peak at 58°C. Despite the liquid polyols displaying the highest melting peak above room temperature, the amount of the crystallizing species needed to gel the whole sample was not sufficient, but they were cloudy.

### Gelation of polyols and MDI systems

The gelation of polyfunctional systems occurs when the branching parameter reaches the critical value. For the reaction mixtures of components containing groups *A* and *B*, according to Flory and Stockmayer,<sup>23</sup> gelation occurs when

$$\alpha_c(f_{aw} - 1)(f_{bw} - 1) = 1 \quad (5)$$

where  $f_{aw}$  and  $f_{bw}$  denote the weight-average functionalities of the *A*-bearing and *B*-bearing reactants,

respectively, and  $\alpha_c = (p_a p_b)_c$  is the critical branching coefficient.  $p_a$  and  $p_b$  are the extents of reaction of *A* and *B* groups. The conversion of OH groups at the gel point,  $p_{ac}$ , for the  $f_{aw}$ -functional polyol and  $f_{bw}$ -functional isocyanate (in our case,  $f_{bw} = 2$ ) at the stoichiometric ratio of OH and isocyanate groups ( $p_a = p_b$ ) is determined with this expression:

$$p_{ac} = \sqrt{\frac{1}{f_{aw} - 1}} \quad (6)$$

The values of  $p_{ac}$  for different soy polyols and MDI were obtained from calculated  $f_w$  values and are given in Table A.II as gel points.

### Monte Carlo simulation of network building

A gelation simulation using the DryAdd program<sup>24</sup> was carried out on soy polyols and MDI systems. The network parameters obtained by the simulation are presented in the appendix in Table A.III. The conversions at the gel point are close to the values in Table A.II obtained from eq. (6) with calculated  $f_w$  values for our polyols. However, cyclization always exists, and it causes a shift of the gel point toward higher conversions. The crosslinking density, as measured by the number-average molecular weights of network chains ( $M_{cn}$ ), varies from 688 to 1993; as measured by the weight-average molecular weight of network chains ( $M_{cw}$ ), it varies from 760 to 3531. The sol fraction for the total conversion and no cyclization varies from 1 to 58%, which is of the same order of magnitude but somewhat larger than the experimental value shown in Table II, indicating that the calculated composition of the functional species is close to the real one. Experimental values are usually lower than true values because the extraction process may not be complete despite the long times.

True number-average network chain molecular weight ( $M_c$ ) values are smaller because of the dangling

TABLE II  
Swelling Parameters of Polyurethane Networks in Toluene

OH number (mg KOH/g)	56	82	115	155	174	206	225
Degree of swelling (volume/initial volume)	6.56	6.33	2.83	2.13	1.88	1.74	1.68
Sol fraction (%)	70.1	66.5	27.2	12.4	7.1	3.0	2.7

chains by about one-third. If the equivalent weight is reduced by one-third, then  $M_{cn}$  should be in the vicinity of 580. Such a crosslinking density with aromatics being one-third of the structure gives glassy polyurethanes, but not a high glass transition. Moreover, dangling chains plasticize the polymer and reduce  $T_g$ .

Figure A.1 (see the appendix) shows the simulated course of reactions with conversions. The simulated values of gel points coincide with the values calculated by eq. (6) from  $f_w$  values as listed in Table A.II.

### Swelling of networks in toluene

The results of swelling experiments are shown in Table II. None of the samples are completely soluble, even those with  $f_n$  below 1, and this raises the question whether epoxy groups participate in crosslinking. Epoxy groups react with isocyanates in the presence of special catalysts to give oxazolidones, but they are not expected to react under the conditions used in this work.

To prove that residual epoxy groups do not react under given experimental conditions, we prepared samples with pure ESO, monoisocyanate (phenyl isocyanate), and tin and amine catalysts (although they were not used in this work). The epoxy group content measured by titration was unchanged after 2 h at 120°C. Gelation occurred only in systems with  $f_w$  greater than 2, and that condition seemed to be satisfied even in polyols with OH numbers below 82 mg KOH/g, even though  $f_n$  was 1.5 or below 1. A graphic

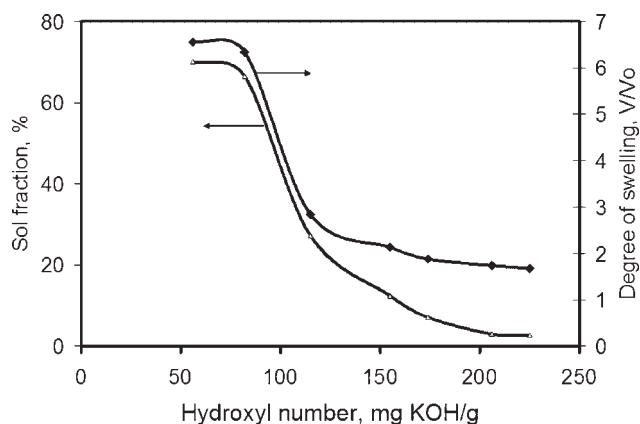


Figure 6 Effect of the OH number of polyols on the degree of swelling and sol fraction of polyurethanes.

representation of the dependence of the swelling degree and sol fraction of polyurethane on the OH number of the polyol is given in Figure 6.

### Thermal and mechanical properties of polyurethanes

The properties of polyurethanes are related to the crosslinking density of the networks, which correlates directly with the OH number of the polyols. Thus, the properties are discussed as a function of the OH number of polyols.

DSC curves of polyurethanes (Fig. 7) show clear glass transitions for samples prepared with polyols having OH numbers of 154 mg KOH/g and higher.

The glass transitions of the samples with OH numbers ranging from 56 to 115 mg KOH/g were not clearly defined because of the high heterogeneity of the samples, the variable degree of the crosslinking density of the network, and the high sol fraction. The polyurethane sample from the polyol with an OH number of 82 displayed melting peaks between  $-40$  and  $0^\circ\text{C}$ , which are characteristic of the melting of ESO; that is, this sample had considerable amounts of unreactive species. The resulting materials were very soft, weak, and rubbery. The properties of the polyurethanes are listed in Table III. Samples made from polyols having OH numbers of 206 and 225 mg KOH/g were glassy, whereas all others were rubbery. The samples with OH numbers of 82 and 56 mg KOH/g were too weak to be tested. The flexural mod-

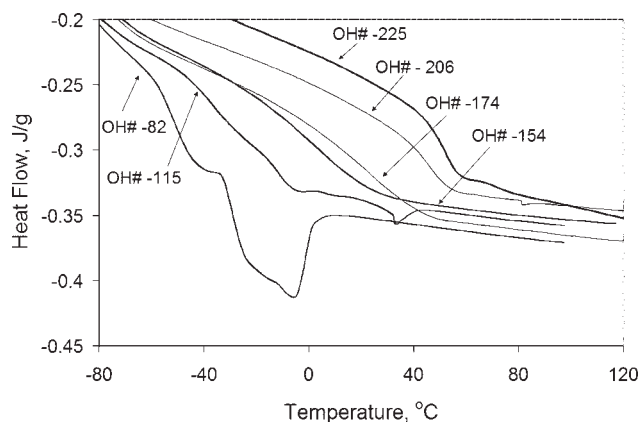


Figure 7 DSC curves of polyurethanes prepared from polyols (with the OH numbers indicated on the curves) and MDI.

**TABLE III**  
**Effect of the Structure of Polyols on the Glass Transitions and Mechanical Properties of Polyurethanes from Partially Hydrogenated ESO Polyols**

Hydrogenation time (h)	0.5	1	2	4	6	16	Fully hydrogenated
Polyol OH number (mg KOH/g)	56	82	115	154	174	206	225
Polyol EOC (%)	5.05	4.34	3.25	2.02	1.36	0.55	0.3
Polyol $f_n$	0.9	1.4	1.9	2.6	2.9	3.5	3.8
$T_g$ by DSC and DMA (°C)			-11 (?) and -13	4.3 (18)	24 (27)	44 (58)	51 (66)
Tensile strength (MPa)			0.4	1.6	12.2	31.4	34.7
Elongation at break (%)			35	42	33	13	8
Shore A hardness			43	68	95	100	100
Flexural modulus (MPa)							626

ulus could be obtained only for the sample prepared with the highest OH number polyol.

Figure 8 displays a linear relationship between the OH number and  $T_g$ , as expected from the Fox–Losheak equation<sup>25</sup> relating the crosslinking density and  $T_g$ :

$$T_g = T_{g\infty} + \frac{K}{M_c} = T_{g\infty} + kv \quad (7)$$

where  $T_{g\infty}$  is the glass transition of the linear polymer of the same structure,  $v$  is the number of crosslinks per unit of volume (density/ $M_c$ ), and  $K$  and  $k$  are constants for a given system. It could be shown that for a complete conversion,  $v$  is directly proportional to the OH number. Higher glass transitions in DMA compared to those from DSC were due to the effect of the frequency and were partly caused by the temperature lag. The DMA values are less ambiguous, but both methods showed the same trend. Two polyurethanes were glassy and the others were rubbery at room temperature. Glassy polyurethanes prepared with polyols having OH numbers of 225 and 206 mg KOH/g displayed moderate strengths.

The tensile strength of polyurethanes increases and the elongation decreases with the crosslinking density and glass transition, as displayed in Figure 9. The first

two samples had very low tensile strengths; the strength was moderate for the rubbery sample with an OH number of 174 mg KOH/g, and the strength was high (30 MPa) for samples having an OH number of 200 and greater. The elongation at break for elastomeric samples was relatively low, never exceeding 45%, indicating that they are fairly imperfect networks because of the low average functionality of the polyols and the absence of oligomers. Heterogeneity in the crosslinking density creates weak points in the structure, as indicated in Figure 10. The flexural modulus of the polyurethane from the fully hydrogenated ESO is 626 MPa, which is characteristic of soft thermoplastics, located between high- and low-density polyethylenes. This fact is related to the relatively low  $T_g$  of this polymer, not far enough from the testing temperature (25°C). The Shore A hardness indicates that the sample with an OH number of 174 mg KOH/g was a hard rubber, and those with lower OH values were soft rubbers. The heterogeneous nature of the crosslinking densities does not affect the properties of the glassy polyurethanes to such a degree as the rubbery samples because intermolecular bonds in the glassy state are strong and control the strength, whereas in the rubbery state they are weak and structural defects are fully exposed.

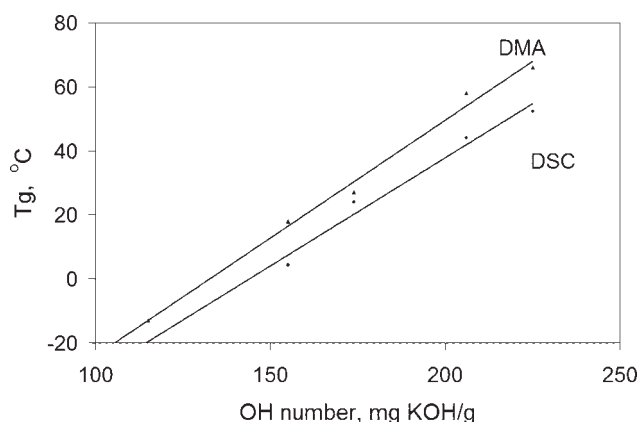


**Figure 8** Effect of the OH number of polyols on the glass transition of polyurethanes determined by DSC and DMA (as maxima on the loss modulus curves).

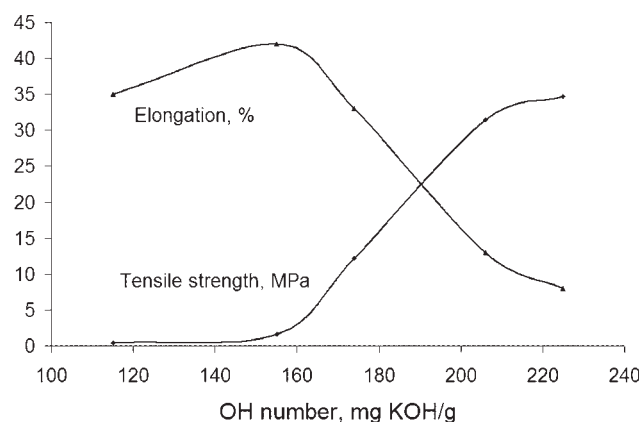
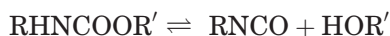


**Figure 9** Effect of the OH number of polyols on the tensile strength and elongation of polyurethanes.



Polyurethanes generally have relatively low thermal stability. Three mechanisms of decomposition of urethane bonds have been proposed:<sup>26</sup>

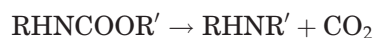
1. Dissociation to isocyanate and alcohol:



2. Formation of a primary amine and olefin:



3. Formation of a secondary amine:



All three reactions may proceed simultaneously. Polyurethanes from vegetable-oil-based polyols with secondary OHs have been found<sup>27</sup> to start degradation below 300°C with activation energies of about 130 kJ/mol. The degradation in our samples also starts somewhat below 300°C by the loss of carbon dioxide from the urethane bond, and this process is faster in polyurethanes from secondary OHs as in our polyurethanes. The thermal stability of polyurethanes as measured by the initial weight loss (Fig. 11) shows a good correlation with the OH number of polyols, increasing with decreasing OH numbers but increasing with the epoxy content in the polyols. The better thermal stability of systems with lower crosslinking density was the opposite of what was found in other soy-based crosslinked polyurethanes without epoxy groups. It appears that

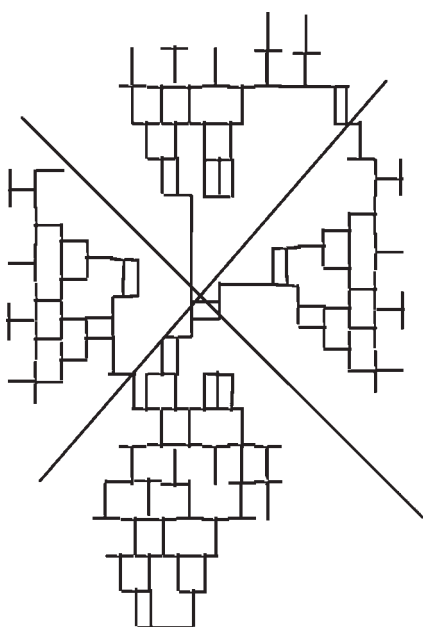


**Figure 10** Schematic representation of a network with a heterogeneous crosslink density. The straight lines indicate probable directions of the fracture propagation.

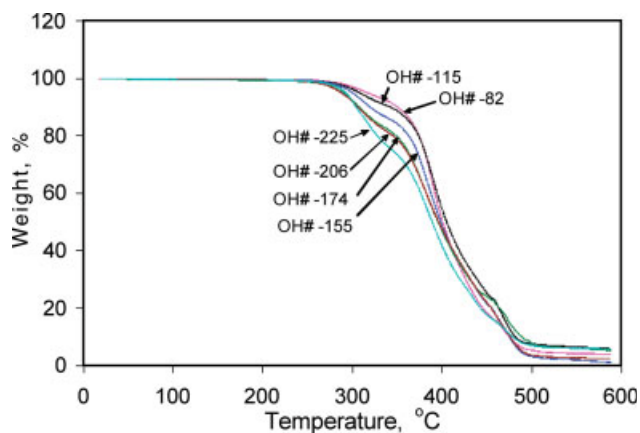


**Figure 11** TGA curves in nitrogen of polyurethanes with different OH numbers. [Color figure can be viewed in the online issue, which is available at [www.interscience.wiley.com](http://www.interscience.wiley.com).]

the residual epoxy groups are good heat stabilizers, although the precise mechanism is not clear.

## CONCLUSIONS

A series of polyurethanes were prepared from polyols obtained by the partial hydrogenation of ESO. The wide distribution of the functional species in the polyols was reflected in the heterogeneity of the crosslinking density of the polyurethanes.

$f_w$  of the polyols varied from 4.4 (OH number = 225 mg KOH/g) to 2.7 for the sample with an OH number of 82 mg KOH/g, indicating that soy-based polyols are strong crosslinkers.

Polyols with OH numbers higher than 150 mg KOH/g were greases or waxes, whereas those with OH numbers of 115 mg KOH/g or lower were liquid at room temperature and were rich in nonfunctional species.

The polyols were virtually monodisperse and displayed very low viscosity in the liquid state in comparison with other polyols from epoxidized vegetable oils.

Polyurethanes prepared from these polyols and diphenyl methane diisocyanate were glassy when the polyol OH numbers were above 200 mg KOH/g and rubbery below that value.

Glassy polyurethanes displayed decent mechanical strengths, whereas rubbery samples showed relatively poor elastic properties characterized by lower elongation and lower strengths, which are characteristic of imperfect, heterogeneous networks. Heterogeneity in the SBO structure, which is directly related to the network structure, is tolerable in highly crosslinked polyurethane systems but negatively affects elastic properties of elastomers.

Polyols prepared by the hydrogenation of ESO show a range of attractive properties, but the tendency to crystallize may limit their attractiveness to industry.

**TABLE A.I**  
**Calculated Properties of Polyols Prepared**  
**by the Hydrogenation of ESO Having Four Epoxy**  
**Groups per Molecule**

Epoxy groups	Molecular weight	OH groups	$E_{OH}$	OH number (mg KOH/g)	EOC (%)
0	946	4	236.5	237.21	0
0.2	946	3.8	248.84	225.44	0.34
0.5	945	3.5	270	207.78	0.85
1.08	944	2.92	323.23	173.56	1.83
1.4	943	2.6	362.77	154.64	2.37
2.07	942	1.93	488.01	114.96	3.52
2.62	941	1.38	681.71	82.29	4.46
3.07	940	0.93	1010.6	55.51	5.23
3.3	939	0.7	1342	41.8	5.62
4	938	0	0	0	6.82

## APPENDIX

### Calculated properties of polyols with Different OH numbers

Properties of polyols from the known ESO can be calculated from the OH and EOC. If we start from ESO with four groups per triacylglycerol, then after hydrogenation, the sum of epoxy groups and OH groups should always be 4. The molecular weight of the oil is about 874, and with the addition of 4 epoxy groups, it increases to  $874 + 4 \times 16 = 938$ . This ESO is the starting material that we used for the preparation of polyols. By the conversion of an epoxy to an OH group, the molecular weight increases by only 2. Thus, the molecular weights of polyols vary only from 938 to 946 or 0.8%; that is, all polyols have practically the same molecular weight. The calculated OH numbers corresponding to our experimental values and other properties of the polyols are given in Table A.I.  $f_n$  of polyols is then equal to the number of OH groups per

triacylglycerol. There are no assumptions in these calculations, and the values are generally correct. The EOC values for a given OH number differ somewhat from the measured EOC values shown in Tables I and III because the measurement of EOC in the presence of OHs is not very precise, especially at low contents of epoxy groups. The deviations could be estimated by the comparison of the experimental values with those calculated in Table A.I

### Calculated compositions of polyols

We have applied a certain algorithm to polyols with reduced OH numbers to calculate their compositions from the composition of the original oil. Typically, the weight fraction with  $f$ -functional groups ( $w_f$ ) after the reduction of the OH number would be equal to  $w_f = aw_{f0} + bw_{f+1} + cw_{f+2} + dw_{f+3}$ , where  $w_{f0}$  is the weight fraction with functionality  $f$  in the starting composition,  $w_{f+1}$  is the weight fraction of species with functionality  $f + 1$ ,  $w_{f+2}$  is the weight fraction of species with functionality  $f + 2$ , and so forth. Coefficients  $a$ ,  $b$ ,  $c$ , and  $d$  are adjusted so that  $a + b + c + d = 1$  and so that the OH number and  $f_n$  are matched with experimental values. For example, if the OH number is reduced from 269 to 206 (the experimental value), Table A.I gives the closest OH value of 207.78 and an  $f_n$  value 3.5; then, each fraction  $w_f$  should be calculated by the multiplication of the original composition with some coefficients, which in this case were found to be  $a = 0.65$ ,  $b = 0.25$ ,  $c = 0.05$ , and  $d = 0$ . This means that 65% of the original fraction of functionality  $f$  is unchanged, but 25% of the fraction with  $f + 1$  is converted to  $f$ -functional species, and about 5% of the  $f + 2$  functional species from the original are added to the  $f$ -functional fraction. The resulting composition of the polyols would have an OH

**TABLE A.II**  
**Simulated Compositions of the Polyols**

		OH number						
		269	225	206	174	155	115	82
Functionality	0	0.18	1.27	3.01	8.41	11.98	20.55	31.91
	1	0.84	5.32	8.51	14.27	17.17	23.77	29.99
	2	5.43	13.70	16.74	19.78	20.96	23.58	20.45
	3	14.68	22.92	22.98	21.61	20.34	17.13	9.59
	4	27.75	23.12	21.83	17.64	15.02	8.82	4.47
	5	20.61	20.11	16.86	11.84	9.49	4.22	2.41
	6	22.95	10.86	8.15	5.25	4.11	1.59	0.98
	7	6.81	2.47	1.76	1.10	0.85	0.31	0.20
	8	0.75	0.22	0.15	0.09	0.07	0.03	0.02
9	0	0.00	0	0	0	0	0.00	
Sum $W_i$		100.00	100.00	100.00	100.00	100.00	100.00	100.00
Gel point (%)		50	54	56	59	61	69	76
$f_n$		4.6	3.8	3.45	3.06	2.59	1.91	1.37
$f_w$		5	4.4	4.18	3.91	3.69	3.11	2.74
$M_n$		945	940	940	940	940	940	940
$M_w$		946	940	940	940	940	940	940

$W_i$ , weight of the fraction  $i$ .

**TABLE A.III**  
**Properties of Polyurethane Networks Obtained from Polyols of Different OH Numbers and MDI with a Monte Carlo Simulation**

OH number	Gel point (% conversion)	Sol fraction (%)	$M_{cn}$	$M_{cw}$	$f_{\text{junction}}^a$
269	50	1.4	688	760	4.70
225	54	4.9	783	965	4.3
206	56	8.3	838	1086	4.1
174	59	15.8	943	1314	3.8
155	61	20.3	1020	1485	3.7
115	69	35.7	1418	2335	3.1
82	76	57.8	1993	3531	2.8

<sup>a</sup> Average junction functionality.

number of 205.93 and an  $f_n$  value of 3.45, which are very close to the targeted values for the OH number and  $f_n$ , but now we have also  $f_w = 4.18$ . The composition values in Table A.II for each polyol are closely related to the known compositions given in the column for an OH number of 269.

In this way, the composition of a polyol is related to the composition of the original oil or ESO, the sum of all fractions is 100%, and each fraction is affected by higher functionality fractions in the original oil (or ESO).

The compositions of the polyols are given in Table A.II. The constant molecular weight of the polyols was taken to be 940, except for the fully hydrogenated theoretical case, for which the true value was calculated to be 946. Because of incomplete conversion, this polyol could not be prepared.

### MONTE CARLO SIMULATION RESULTS

Gelation simulation using the DryAdd program was carried out on soy polyols and MDI systems. The sample size was set to 200,000 molecules. Assuming total conversion and no cyclization, the

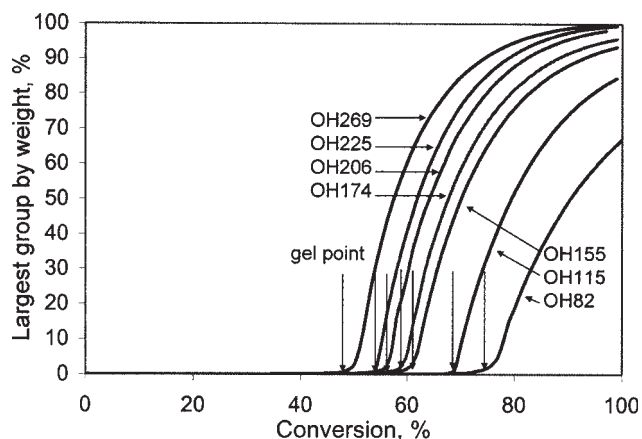


**Figure A.1** Dependence of the largest molecule (gel) content on the conversion.

simulation gave network parameters, as listed in Table A.III. Gel points are identified as the departure from the  $x$  axis on curves of the largest group versus the conversion.

Figure A.1 shows the simulated course of reactions with the conversions. The gel points are located at 50–76% conversions. The largest group in the simulation represents the gel. Figure A.1 also shows that the amount of gel in the final product (100% conversion) decreases as the OH number decreases. The average functionality of the junctions in the network, calculated as two junctions times the number of network chains divided by the number of branch points, correlates well with the polyol  $f_w$  value.

### References

- Holcapek, M.; Jandera, P.; Zderadicka, P.; Hrubá, L. *J Chromatogr A* 2003, 1010, 195.
- List, G.; Stedley, K. R.; Neff, W. E. *Inform* 2000, 11, 980.
- Guo, A.; Cho, Y.-J.; Petrović, Z. S. *J Polym Sci Part A: Polym Chem* 2000, 38, 3900.
- Zlatanić, A.; Lava, C.; Zhang, W.; Petrović, Z. S. *J Polym Sci Part B: Polym Phys* 2004, 42, 809.
- Guo, A.; Demydov, D.; Zhang, W.; Petrović, Z. S. *J Polym Environ* 2002, 10, 49.
- Petrović, Z. S.; Zhang, W.; Javni, I. *Biomacromolecules* 2006, 6, 713.
- Javni, I.; Zhang, W.; Petrović, Z. S. *J Appl Polym Sci* 2003, 88, 2912.
- Standard Methods for the Analysis of Oils, Fats and Derivatives; Paquot, C.; Hautfenne, A., Eds.; Blackwell: London, 1987.
- Daute, P.; Stoll, G. (to Henkel K.-G.a.A.). *Eur. Pat.* 584629; WO 9101291 (1991).
- Mel'nik, L. V.; Kurchevskaya, N. V.; Kryukov, S. I. *Khim Prom* 1996, 694.
- Daute, P.; Gruetzmacher, R.; Hoefer, R.; Westfechtel, A. *Fett Wissenschaft Technol* 1993, 95, 91.
- Rowland, S. P.; Conyne, R. F. (to Rohm & Haas Co.). *U.S. Pat.* 2,822,368 (1958).
- Zhao, X. (to Shenzhen Ocean Power Corp.). *Chin. Pat.* CN 1,522,841 (2003).
- Worschech, K.; Loeffelholz, F.; Wedland, P.; Wegemund, B. (to Henkel K.-G.a.A.). *Ger. Pat.* DE 3420226; *Eur. Pat.* 166201 (1985).
- Monteavaro, L. L.; Silva, E. O. D.; Costa, A. P. O.; Samios, D.; *J Am Oil Chem Soc* 2005, 82, 365.
- Plochocka, K.; Dragowska, E. *Polimery* 1972, 7, 367.
- Meffert, A.; Kluth, H. (to Henkel Corp.). *U.S. Pat.* 4,886,893 (1989).
- Kluth, H.; Meffert, A. (to Henkel Corp.). *U.S. Pat.* 4,508,853 (1985).
- Dušek, K.; Dušková-Smrčková, A.; Zlatanić, A.; Petrović, Z. *ACS-PMSE: Orlando*; 2002.
- Zlatanić, A.; Petrović, Z. S.; Dušek, K. *Biomacromolecules* 2002, 3, 1048.
- Hofer, K.; Johari, G. P. *Macromolecules* 1991, 24, 4978.
- Ilavský, M.; Dušek, K. *Macromolecules* 1986, 19, 2139.
- Accelrys Manual, Chapter 7 Networks, Release 4.0.0P, April 1998. <http://www.esi.umontreal.ca/accelrys/materials/insight400P/polymer/07-Netw.doc.html>, accessed March 23, 2007.
- DryAdd Pro+; Intelligensys: Yorkshire, UK, 2003.
- Fox, T. G.; Loshaek, S. J. *J Polym Sci* 1955, 15, 371.
- Saunders, J. R. *Rubber Chem Technol* 1959, 32, 337.
- Javni, I.; Petrović, Z. S.; Guo, A.; Fuller, R. *J Appl Polym Sci* 2000, 77, 1723.